Since January 2020 Elsevier has created a COVID-19 resource centre with free information in English and Mandarin on the novel coronavirus COVID-19. The COVID-19 resource centre is hosted on Elsevier Connect, the company's public news and information website.

Biomedical Signal Processing and Control 83 (2023) 104724

Contents lists available at ScienceDirect

Biomedical Signal Processing and Control

journal homepage: www.elsevier.com/locate/bspc

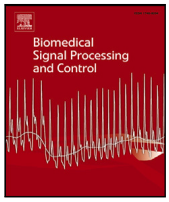

Broad learning solution for rapid diagnosis of COVID-19

Xiaowei Wang [a], Liying Cheng [a,*], Dan Zhang [b], Zuchen Liu [a], Longtao Jiang [a]

[a] School of Physical Science and Technology, Shenyang Normal University, Shenyang, 110034, China
[b] Navigation College, Dalian Maritime University, Dalian, 116026, China

ARTICLE INFO

Keywords:
Broad learning system
COVID-19 diagnosis
CT image
Feature fusion

ABSTRACT

COVID-19 has put all of humanity in a health dilemma as it spreads rapidly. For many infectious diseases, the delay of detection results leads to the spread of infection and an increase in healthcare costs. COVID-19 diagnostic methods rely on a large number of redundant labeled data and time-consuming data training processes to obtain satisfactory results. However, as a new epidemic, obtaining large clinical datasets is still challenging, which will inhibit the training of deep models. And a model that can really rapidly diagnose COVID-19 at all stages of the model has still not been proposed. To address these limitations, we combine feature attention and broad learning to propose a diagnostic system (FA-BLS) for COVID-19 pulmonary infection, which introduces a broad learning structure to address the slow diagnosis speed of existing deep learning methods. In our network, transfer learning is performed with ResNet50 convolutional modules with fixed weights to extract image features, and the attention mechanism is used to enhance feature representation. After that, feature nodes and enhancement nodes are generated by broad learning with random weights to adaptly select features for diagnosis. Finally, three publicly accessible datasets were used to evaluate our optimization model. It was determined that the FA-BLS model had a 26–130 times faster training speed than deep learning with a similar level of accuracy, which can achieve a fast and accurate diagnosis, achieve effective isolation from COVID-19 and the proposed method also opens up a new method for other types of chest CT image recognition problems.

1. Introduction

Globally, the COVID-19 pandemic is causing concern for humanity's survival and has greatly impacted society, medicine, economy, especially with the increasing medical burden [1], rapid and accurate diagnosis is essential to control the spread of an epidemic. Reverse transcriptase polymerase chain reaction (RT-PCR) is considered the standard for timely diagnosis of COVID-19 infections. However, RT-PCR has low accuracy and a long cycle, requiring multiple tests to confirm the results [2]. Shortening the critical period from diagnosis to confirm infection can greatly control the spread of the epidemic and protect people's health.

The use of computer-aided diagnostic devices can detect minute differences that are not detectable by the human eye [3]. They have taken an irreplaceable place in the diagnosis of chest disease. The use of chest CT scans as a quick and accurate COVID-19 screening approach has been demonstrated [2,4]. Rapid availability of results with CT imaging in the emergency setting may be utilized before receipt of RT-PCR results to prevent false negative reporting. However, the increased number of COVID-19 patients places a heavy strain on manual diagnosis, and the precision of the diagnosis results cannot be guaranteed, putting patients at the danger of infection [5,6].

In order to detect COVID-19, the deep convolutional neural network (DCNN) approach has been developed, which will help doctors diagnose COVID-19. Mortani Barbosa et al. used logistic regression and random forest to interpret features to achieve automated diagnosis of COVID-19 in large multicenter cohorts, and conducted experiments on a dataset consisting of 2446 chest CT scans [7]. Wang et al. used CNN to extract specific graphic features for CT image screening of COVID-19, analyzed 1065 representative images examined by two radiologists and achieved 89.5% detection accuracy in the case of a small-scale dataset [8]. [9] proposed a deep model with for COVID-19 diagnosis, creating an experimental dataset from 852 CT scans and discussed the results with advanced supervised learning methods. Currently, studies on COVID-19 detection with small-scale datasets still account for a large proportion [10], but deep learning models cannot perform better without access to high-quality data [11]. Small-scale datasets can reduce the burden of models and hardware devices, but how to use small data to achieve better model performance is still a problem to be solved. [12] comprehensively explained the deep model from different angles, and

* Corresponding author.
E-mail address: clypzb@163.com (L. Cheng).

https://doi.org/10.1016/j.bspc.2023.104724
Received 8 September 2022; Received in revised form 27 January 2023; Accepted 14 February 2023
Available online 17 February 2023

applied the architecture to COVID-19 diagnosis, forming a dataset of 6233 CT images to evaluate and explain the diagnosis model. [13] proposed a 3D convolution network to evaluate the performance of COVID-19 recognition in a large-scale dataset containing 4982 CT images. In order to accomplish precise recognition and reliable feature extraction, [14] added three more layers to the ResNet50 architecture, using 5427 infected COVID-19 and 2628 healthy CT images evaluation model. There are also studies that select large-scale datasets for multi-classification tasks [15–18]. However, due to the complexity of the deep learning model and the high hardware necessities [11], the price of medical instrumentality can directly increase. Moreover, thanks to the continual change of the disease, the model often needs to be retrained to adapt to the CT characteristics of patients in the current time or region, the delay of detection results leads to the spread of infection and an increase in healthcare costs. In order to effectively detect coronavirus infection and deal with the unbalanced economic development in various regions, it is necessary to develop a simple, efficient and economical application.

On the basis of breaking through these problems, we propose a novel diagnostic method for COVID-19 by combining deep and broad neural networks. (1) Transfer learning can be effectively to handle a small-scale public dataset [19], which uses network weights trained on a large general dataset to extract data features of the application domain. We can get good characteristic representations through transfer learning. (2) In response to the need for rapid COVID-19 diagnosis, we provide a broad learning system as an alternative to DCNN to provide the performance of rapid diagnosis. Convolutional networks are used in feature extraction and broad learning is used in fast diagnosis in our method. Feature extraction model improve the accuracy of using existing small-scale datasets. Because broad learning is a single-layer network with fewer parameters, the complexness of the network is greatly reduced compared with the deep model. The FA-BLS for COVID-19 diagnosis can reduce the training time by 26–130 times compared with other algorithms, and has the similar level of accuracy as deep network. The main contributions of this study are as follows:

- We propose a new end-to-end model (FA-BLS) as an alternative to complex deep learning for COVID-19 diagnostic task with small-scale datasets.
- This method can extract image features more effectively. It uses ResNet50 with generalization feature extraction ability after pre-training to extract features, so as to reduce the impact of randomly generated weights in BLS on performance and extract rich discrimination information.
- We conducted a comprehensive experimental evaluation of the model and selected three publicly available datasets for validation to demonstrate the rapidity and accuracy of our technique. The results demonstrate that the speed of FA-BLS is greatly improved with comparable accuracy.

2. Related works

In this section, we discuss the following aspects that are closely related to our work: transfer learning and feature extraction, broad learning system and artificial intelligence for COVID-19.

2.1. Transfer learning and feature extraction

Transfer learning (TL) is the process of transferring the learned and trained model parameters to a new model [20]. In image processing, TL mainly uses a large general dataset to obtain fixed weights, and uses the weights to extract data features from the dataset of the object under study. In special cases such as epidemic outbreaks, it is difficult to obtain large public datasets, so TL is popular for small-scale dataset tasks [11]. Wang et al. proposed a chest image classification model using pre-trained deep networks for transfer learning and added an attention module [21]. Li et al. proposed objective metaplasia (GIM) recognition model based on transfer learning, which uses different modules to learn feature weights and then perform feature fusion [22]. In the study by Ahuja et al. four different pre-trained CNN models are utilized to detect COVID-19 [23]. By combining 15 pre-trained CNN architectures with an ensemble method based on transfer learning, Gifani et al. further improved the recognition ability of COVID-19 [24].

Although the pre-trained weights on the ImageNet dataset can effectively extract data features, not all features contribute to the classification work, and the attention mechanism can help extract meaningful features from many features [25]. [26] propose a “Residual Attention Network”, which uses the attention-aware function generated by the attention module for image classification. Zhou et al. combined U-net with attention mechanism, used re-weighted features to better-acquired features, and proved the effectiveness of attention mechanism [27]. [28] propose prior-attention strategy to highlight diseased regions in the lung for COVID-19 diagnosis. [29] innovatively fused CT and X-ray images and demonstrated that convolutional attention modules have a positive effect on diagnostic accuracy. In response to the loss of detail, Xia et al. extract semantic information around the target by introducing multi-scale and context attention modules [30]. Inspired by the above work, we add an attention mechanism and transfer learning to the diagnosis network to improve the network performance for the feature extraction problem with limited datasets.

2.2. Broad learning system

Broad learning (BL) [31] is evolved on the basis of random vector functional-link neural network (RVFLNN). BL with a single layer network structure was proposed as an alternative to DCNN, BL can use fewer neurons to achieve higher test recognition accuracy [32]. BLS has been widely utilized in various fields due to its fast learning ability [33–35], such as image recognition [36,37], classification and regression [38], and data modeling [39]. Although BL has achieved the most advanced performance in many applications, the original BLS still has many limitations when dealing with complex tasks. It uses arbitrary continuous probability distribution to randomly generate node weights, which cannot effectively extract the deep features of the image and is not suitable for the pathological diagnosis task of chest CT images. Therefore, in this study, we used convolutional networks to capture more features to make up for the shortage of BL, and then BL was utilized to efficiently diagnose COVID-19.

2.3. Artificial intelligence for COVID-19

Artificial intelligence has made considerable strides in image processing over the past few years. In the field of medical image processing, AI can effectively classify different images to assist diagnosis and reduce the rate of misdiagnosis. [40] proposed a lightweight neural network framework called COVID-Net, which improves the transparency and reliability of predictions and proposes an open benchmark X-ray image dataset. Gozes et al. combine deep models of different dimensions with clinical understanding to enable automated diagnosis of COVID-19 [41]. Shan et al. achieve a precise description of COVID-19 condition by quantifying infected area [42]. Kollias D et al. introduced a new large CT scanning database and used CNN-RNN architecture for COVID-19 diagnosis [43]. In [44], visual features were extracted from the image to distinguish COVID-19 from community-acquired pneumonia and healthy individuals. Fan et al. propose a semi-supervised deep network (Inf-net) to segment pulmonary infection by combining parallel decoder and attention mechanism [45]. It turns out that the convolutional layer in DCNN is very suitable for extracting these features from images.

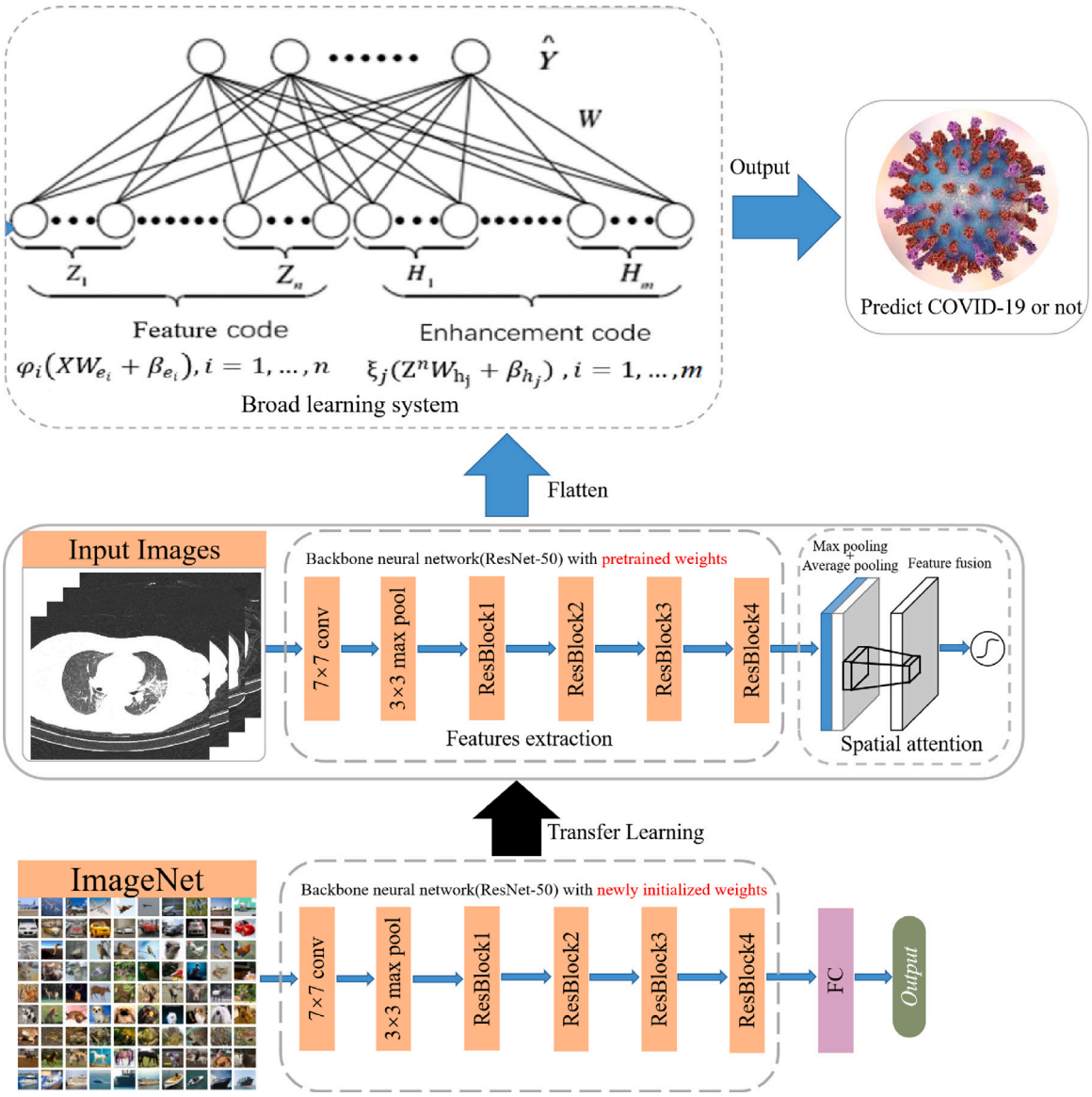

Fig. 1. The architecture of our proposed FA-BLS.

3. Methods

In this section, we introduce FA-BLS in detail from the perspective of network structure and constituent modules. In our work, we combined transfer learning, attention mechanism and BLS to perform the diagnostic. Firstly, the original CT images were input to the feature fusion module with attention mechanism to efficiently extract the image features. Then the extracted features are input into BLS, and the speedy diagnosis is achieved through randomly generated functional nodes. The following subsections describe each part in detail.

3.1. Framework

The network framework we proposed is shown in Fig. 1. This system includes two parts, the feature fusion module is used for feature extraction and feature fusion, and we add the spatial attention module to strengthen the target area. The extracted features are then sent to the BLS for definitive diagnosis.

3.2. Feature extraction module based on residual attention mechanism

Feature extraction is the elementary work of image extraction. It can be seen from the aforementioned article that the convolutional layer in DCNN is very suitable for extracting these features from images. Therefore, in our network FA-BLS, for the case where the dataset is difficult to obtain, we use ResNet50 for feature extraction. As shown in Fig. 2, the backbone network ResNet50 [46] is pre-trained on ImageNet to obtain weights with generalization ability, which are used to extract COVID-19 features in the form of transfer learning.

ResNet50 stands for 50-layer residual network, which uses the residual structure of skip connection and implements identity mapping between layers, enabling the network to achieve better performance with an increased number of layers of the convolutional network. Compared with CNN stacked by other convolutional layers, it addresses the problems of insufficient training data and deep network degradation to a certain extent. The ResNet50 convolution module, pre-trained based

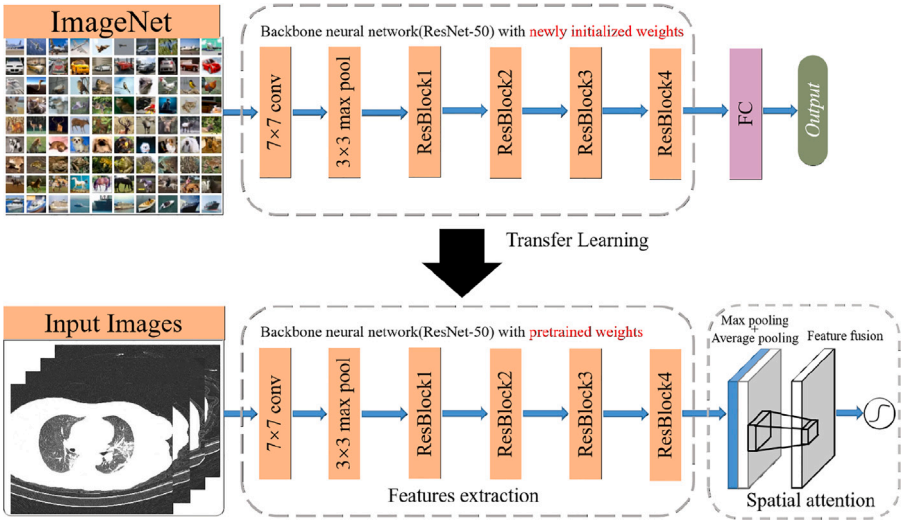

Fig. 2. Structural diagram of feature attention fusion module.

on a large dataset Imagenet, despite efficient extraction of generalization features, has degraded the performance of the model in the target domain due to the particularities of medical images. The introduction of attention mechanism can provide performance improvements to models by assigning more weight parameters to important features, and using this mechanism feature extraction module could retain more important information and reduce the interference caused by redundant content to the network.

The spatial attention module (SAM) utilizes two pooling operations to generate two 2-dimensional features for channel information of feature maps. SAM is based on the global average pooling channel as well as the global biggest pooling operation, produced two represent different characteristics of figure, the merged by another larger receptive field 7×7 convolution of feature fusion, and then the weight graph is generated by operation and combined with the features extracted in the previous step so that the target area can be strengthened. The formula for calculating SAM is:

$$\begin{aligned} M_s(F) &= \sigma(f^{7x7}([AvgPool(F)]; [MaxPool(F)])) \\ &= \sigma(f^{7x7}([F_{avg}; F_{max}])) \end{aligned} \tag{1}$$

3.3. Broad learning system

The biggest difference between broad learning and deep learning lies in the number of network layers and the way of data processing. Fig. 3 shows the differences between the two image processing methods. CNN uses a convolution kernel of appropriate size to extract features by calculating pixels of each image one by one. While BL stretches each image pixel into a row, all pixels collectively make up a large matrix for operation, which makes BL's model complexity greatly reduced compared to DL, and operation speed improved significantly. But single-layer network which is concise and efficient also brings some disadvantages, it cannot extract image deep features like a convolutional neural network, so this research combined CNN with BL to synthesize the advantages of both for better performance of detection tasks.

The structure of the system is shown in Fig. 4. The input, feature node, enhancement node, and output make up the entire network. In this section, the output of the feature extraction layer will be used as the input matrix X of BLS, then $X = [x_1, \ldots, x_n]^T \in R^{N \times B}$,output $Y = [y_1, \ldots, y_n]^T \in R^{N \times C}$, N represents the total number of samples, B represent the dimension of samples, C represents the total number of classes.

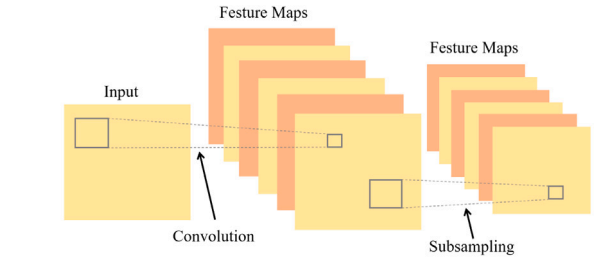

(a) Data processing of convolutional neural network

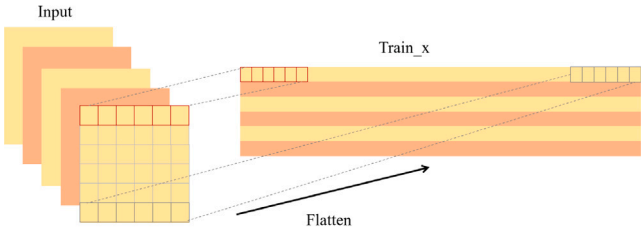

(b) Data processing of broad learning

Fig. 3. Data processing with different structures.

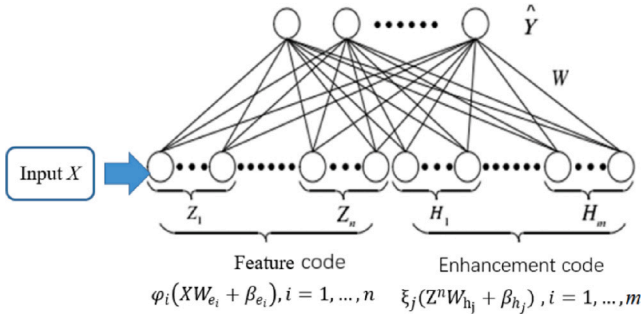

Fig. 4. The model structural of broad learning networks.

For n feature maps, each map generates n nodes, then the ith feature node can be expressed as follows:

$$Z_i = \varphi_i(XW_{e_i} + \beta_{e_i}), i = 1, \ldots, n \tag{2}$$

Where W_{e_i} and β_{e_i} are both randomly generated weights and offsets,Since φ is a linear activation function, the mapping feature is linear. The sparse autocoding method is used by BLS to optimize the input weights in order to get over the unpredictable nature of random initialization.

$Z^n \equiv [Z_1, \ldots, Z_i]$ is used to symbolize each feature node, and for m enhanced nodes, the jth enhanced node can be expressed as:

$$H_j \equiv \xi_j(Z^n W_{h_j} + \beta_{h_j}), j = 1, \ldots, m \tag{3}$$

ξ is a nonlinear activation function where Typically, it can be configured as a hyperbolic tangent function:

$$\xi(x) = tanh(x) \tag{4}$$

All enhancement nodes are represented as $H^m \equiv [H_1, \ldots, H_j]$, therefore, the BLS model can be expressed as the following equation:

$$\begin{aligned} Y &= [Z_1, \ldots, Z_i][\xi(Z^n W_{h_1} + \beta_{h_1}), \ldots, \xi(Z^n W_{h_j} + \beta_{h_j})]W \\ &= [Z_1, \ldots, Z_i][H_1, \ldots, H_j]W \\ &= [Z^n \mid H^m]W \end{aligned} \tag{5}$$

Where $W = [Z^n \mid H^m]^+$ is the connection weight between the hidden layer of the broad structure and the output layer. W_{e_i}, β_{e_i}, W_{h_j} and β_{h_j} are all functional nodes randomly generated and fixed throughout the whole process. By solving the ridge regression approximation of $[Z^n \mid H^m]^+$, W can be easily computed.

We choose L2-norm regularization to solve this optimal problem, which has convexity and good generalization performance. The objective function of BLS is:

$$argmin(\|Y - \hat{Y}\|^2 + \frac{\lambda}{2}\|W\|^2) \tag{6}$$

Where, λ is the regularization coefficient, and $\hat{Y}$ is the prediction result, it is easy to obtain:

$$W = (A^T A + \lambda I)^{-1} A^T Y \tag{7}$$

The identity matrix is denoted by I in the equation, while A^T represents A permutation and A pseudo-inversion is denoted by $A^+ = \lim_{x \to 0}(A^T A + \lambda I)^{-1} A^T$, formula (7) can be written as $W = A^+ Y$.

For the label Y, y_i represents the probability that the system predicts each category, which can be defined as

$$\hat{y}_i^j(x_i) = \frac{y_i^j(x_i) - min_{B \in 1,2,\ldots,C} y_i^B(x_i)}{\sum_{B=1}^{C} y_i^B(x_i)} \tag{8}$$

Finally, the probability output is

$$\hat{y}_i(x_i) = \begin{pmatrix} \hat{y}_i^1(x_i) \\ \vdots \\ \hat{y}_i^C(x_i) \end{pmatrix} \tag{9}$$

4. Experiments and analysis

In this section, we conduct a series of experiments to demonstrate the effectiveness of the planned FA-BLS in COVID-19 diagnosis.

4.1. Data description

In this paper, we select three publicly available COVID-19 datasets to obtain more reliable evaluation results (as shown in Table 1). Fig. 5 indicates the CT images of COVID-19 patients and non-infected cases.

- CC-CCII [47] is obtained from the China Consortium of Chest CT Image Investigation. All images were divided into novel coronavirus pneumonia (NCP) caused by SARS-CoV-2 virus infection, common pneumonia and a normal control group, 750 with labels are selected for study in this paper.

Table 1
A summary of public COVID-19 imaging datasets.

Datasets	Total	COVID-19	Non COVID-19
CC-CCII	750	549	201
COVID-CT-Dataset	812	349	463
SARS-COV-2	2482	1252	1230

Table 2
Confusion matrix representation.

Actual	Predicted	
	Yes	No
Yes	TP	FN
No	FP	TN

Where TP denotes "True Positive", TN denotes "True Negative", FN represents "False Negative", and FP represents "False Positive".

- COVID-CT-Dataset [48] is collected from COVID19-related papers from medRxiv, bioRxiv, NEJM, JAMA, Lancet, etc. It includes 349 CT scans with COVID-19 and 463 CT scans without COVID-19, and a senior radiologist confirmed the validity of the dataset.
- SARS-CoV-2 dataset [49] is a public CT scanning dataset constructed by Soares and others, including 1252 CT images infected with COVID-19 and 1230 CT images uninfected with COVID-19, with a total of 2482 CT images. These datas was collected from actual patients in hospitals.

4.2. Evaluation metrics

The comparison of diagnostic test results with the gold standard can reflect the pros and cons of diagnostic methods. Some evaluation indicators are commonly used in medical diagnosis, this paper selects the following popular indicators to evaluate our method: Accuracy(Acc), Sensitivity(Sen) and Specificity(Spec). They are defined as follows. A confusion matrix is represented as in Table 2.

$$Accuracy = \frac{TP + TN}{TP + FP + TN + FN} \tag{10}$$

$$Sensitivity = \frac{TP}{TP + FN} \tag{11}$$

$$Specificity = \frac{TN}{TN + FP} \tag{12}$$

4.3. Implementation details

We did our experiments in Python 3.6, the process runs on a 2.2 GHz Core i5 processor with 4 GB of RAM. All datasets are divided into training and testing datasets according to 8:2, and the final evaluation results are obtained through five-fold cross-validation. Bayesian optimization is employed to optimize the hyperparameters during our technique. The hyperparameters of the BLS principally embrace the quantity of feature windows (N1 = 100), the number of nodes within each feature window (N2 = 8) and the number of enhancement nodes (N3 = 2084).

4.4. Quantitative analysis

In this section, FA-BLS is compared with the classical DCNN method to prove its rapidity. To quantify the improved effect of FA-BLS, the same hyperparameters are used to train the ordinary BLS. Some classic deep CNN, such as VGG16 [50], ResNet50, Xception [51] and Efficientnet [52] also use the same hyperparameters as ResNet50 in feature fusion layer(Batch size = 16, Optimizer = Adam, Activation function = Softmax, Loss function = Binary crossentrop). Meantime, the weights

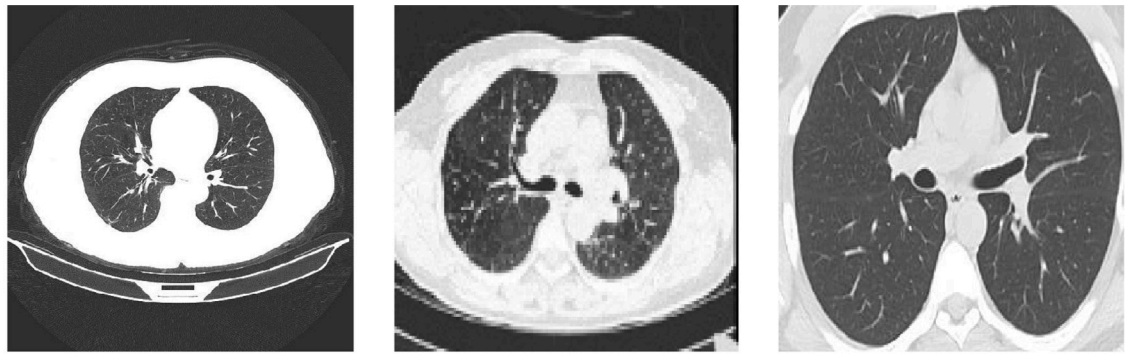

(a) Non COVID-19

(b) COVID-19

Fig. 5. CT images of healthy and patients with COVID-19 pneumonia. The red clippers represent a typical ground-glass opacity (GGO) in the area affected by COVID-19.

Table 3
Classification results of each algorithm in CC-CCII dataset under the same hyperparameter.

Models	Training Acc (%)	Testing Acc (%)	Training time (s)
ResNet50	93.68	92.80	24246.13
Xception	90.42	88.63	45440.04
Efficientnet	88.58	87.11	27345.64
VGG16	95.60	93.32	9147.86
BLS	84.72	65.33	56.29
FA-BLS	99.31	93.93	363.34

Table 4
Five cross-validation classification results of each algorithm in CC-CCII dataset.

Models	Training Acc (%)	Testing Acc (%)	Training time (s)
ResNet50	95.71	93.80	26531.34
Xception	96.35	92.18	47361.70
Efficientnet	93.06	90.85	28909.14
VGG16	96.45	93.79	9682.35
BLS	89.64	69.58	68.13
FA-BLS	99.31	93.93	363.34

Table 5
Five cross-validation classification results of each algorithm in COVID-CT-Dataset.

Models	Training Acc (%)	Testing Acc (%)	Training time (s)
ResNet50	96.12	94.15	25970.47
Xception	95.97	92.54	50672.64
Efficientnet	93.47	91.12	30788.08
VGG16	97.20	94.25	10359.15
BLS	87.69	69.25	75.62
FA-BLS	99.42	93.98	378.24

Table 6
Five cross-validation classification results of each algorithm in SARS-CNV-2 dataset.

Models	Training Acc (%)	Testing Acc (%)	Training time (s)
ResNet50	97.82	94.53	71416.52
Xception	98.52	94.21	141374.88
Efficientnet	95.17	92.34	86514.28
VGG16	98.15	93.860	29007.27
BLS	89.82	71.11	253.24
FA-BLS	99.47	94.05	998.25

of all methods are obtained by pre-training ImageNet, and the training of deep learning is performed only around the last layer. In Table 3, the classification results of each method under CC-CCII dataset are given. The accuracy of ordinary BLS identification is only 65.3%, far lower than that of classical DCNN, but the accuracy of FA-BLS proposed by us reaches 93.9%, 28.6% higher than that of ordinary BLS in the case of small-scale datasets. DCNN runs a long time period thanks to additional parameters, but our FS-BLS introduces a broad structure to reach high identification accuracy with few parameters for limited datasets.

For ordinary BLS and different deep convolutional neural networks, setting the same hyperparameters as our model cannot show the best performance of the network, and may also produce an overfitting phenomenon. We selected appropriate hyperparameters for each network to more objectively evaluate the performance results of our model as shown in table Tables 4 to 6. The deep network has achieved better performance improvement at the cost of training time, but it can be observed from the table that the network improvement of DCNN under the small-scale datasets is still not ideal, just achieving the same level of performance as FA-BLS. A key challenge for deep networks is that the total amount of data in this task is too small to meet the needs of network learning, so even using the most appropriate hyperparameter will not achieve the excellent performance of deep models under large dataset tasks. In contrast to this, the training time of FA-BLS is significantly reduced compared with that of the deep network. It is 130 times faster than the Xception network and 66 times faster than ResNet50 while processing the same data. In the deep model, VGG16 provides

Table 7
Compare our results with other advanced algorithms.

Research group	Dataset used	Technique	Overall Acc (%)	Sen (%)	Spec (%)
Wang et al. [8]	C-19: 740 NC: 325	Inception	89.5	88	87
Pathak et al. [9]	C-19: 413 NC: 439	ResNet50	93.02	94.78	91.46
Li et al. [53]	C-19: 1980 NC: 1164	Efficientnet	93.46	90.57	90.87
Altan et al. [54]	C-19: 142 NC: 142	VGG16	–	97.62	78.57
Oluwasanmi et al. [55]	C-19: 700 NC: 700	ResNet50 + VGG16	94.00	96.00	92.00
FA-BLS(CC-CCII)	C-19: 549 NC: 201	ResNet50 + BLS	93.93	91.23	90.61
FA-BLS(COVID-CT-Dataset)	C-19: 349 NC: 463	ResNet50 + BLS	93.98	92.13	91.60
FA-BLS(SARS-CNV-2)	C-19: 1252 NC: 1230	ResNet50 + BLS	94.05	92.57	91.92

Table 8
Diagnosis accuracy of different mapping parameters.

Feature nodes	Enhancement nodes	Testing Acc (%)	Training time (s)
64×8	2000	89.33	126.45
100×8	200	92.73	252.07
100×8	800	92.96	256.13
100×8	1200	93.25	170.62
100×8	2000	93.50	298.29
100×16	2000	92.73	421.42
100×32	2000	93.24	271.29
100×64	2000	93.30	243.42
200×8	2000	93.68	188.07
500×8	2000	93.91	140.07
1000×8	2000	92.83	967.50

better results, as it trains fewer parameters and takes less time to train samples. The proposed model has similar performance compared to the competing model, but when we applied the proposed model to larger populations, the algorithmic speed increase could keep more people from getting sick.

4.5. Effectiveness analysis

To prove the effectiveness of the planned framework, the analysis results of the planned framework and other advanced classifiers used to observe COVID-19 were compared in Table 7, where C-19 denotes "COVID-19", NC denotes "Non COVID-19". The reported results for the comparator methods were taken from their papers as we were unable to reproduce their codes. The performance of each model was estimated according to three different variables: accuracy, specificity and sensitivity. At present, most classification researchers seek to improve the performance, but seldom report the model training time in the paper. Therefore, this section does not discuss speed, focusing on the performance comparison of our model with other advanced methods.

The results show that our study can distinguish between COVID-19 positive and healthy patients who are not infected, a potential reason being that our feature fusion module provides robust feature representation. In terms of ACC, the use of multiple datasets also further ensures the credibility of our proposed COVID-19 diagnosis model. It can be seen from the Table 7 that when the total amount of data is similar, the classification accuracy of our method has significantly improved compared with the network using ResNet50 only [9]. In addition, our strategy of combining ResNet50 with BLS and the method of combining two deep models [55] have achieved approximate performance. However, from the discussion of training time in the previous section, it is known that our model has considerable advantages in terms of training speed. The evaluation results of FA-BLS performance with three datasets show that the size of input data has little impact on the performance of this method, as an auxiliary diagnostic tool, our proposed method may serve as a reliable clinical adjunct to COVID-19 diagnosis.

4.6. Broad learning parameter analysis

For additional study the classification performance of FA-BLS, we have a tendency to explore the influence of various variety of functional nodes on the experimental results, as shown in Table 8. It is obvious that with the rise of the amount of nodes, the training time progressively becomes longer, however, it is not the model with more nodes that has higher classification accuracy. The selection of nodes is the determinant of the experimental accuracy.

5. Conclusion

By analyzing chest CT images, a new model(FA-BLS) for the diagnosis of COVID-19 is developed, which can accurately classify images. Our approach utilizes a broad structure to improve diagnosis speed and alleviate the shortage of high-quality label data through transfer learning. In this paper, we used three publicly available datasets with a total of 4044 CT images for testing and training. In the experimental results, we have proved the effectiveness of the proposed method in CT image diagnosis of COVID-19. Our network gets the advantages of a simple structure, significantly reduced parameters and low hardware requirements, so it has great application potential in the diagnosis of COVID-19. Compared with DCNN, this method has less calculation and faster training speed than 26 times. This model can achieve the same level of accuracy as the deep learning model under the small-scale dataset task, and make up for the shortcomings and weaknesses of the recognition task based on deep learning.

Our network provides clinical value in two aspects: (1) During the speedy spread of COVID-19, it will get the diagnosis result quicker than RT-PCR and DCNN, which might effectively cut down the spread. (2) Our model has low requirements for hardware, which helps to popularize in a large area. It is more suitable for replacing expert doctors to complete the diagnosis of COVID-19 independently in rural areas with limited resources, and effectively reduces the medical burden of the government on the premise of ensuring accuracy. At the same time, the proposed method opens up a new method for other types of chest CT image recognition, and also provides guidance for the accurate recognition of small group diseases and regional diseases based on CT images.

CRediT authorship contribution statement

Xiaowei Wang: Writing – original draft, Validation, Formal analysis, Visualization, Software, Methodology. **Liying Cheng:** Methodology, Writing – review & editing, Resources, Supervision, Project administration. **Dan Zhang:** Resources, Formal analysis. **Zuchen Liu:** Investigation, Validation, Software. **Longtao Jiang:** Investigation, Validation, Software.

Declaration of competing interest

The authors declare that they have no known competing financial interests or personal relationships that could have appeared to influence the work reported in this paper.

Data availability

The authors are unable or have chosen not to specify which data has been used.

References

[1] M. Miller, Novel coronavirus COVID-19 (2019-nCoV) data repository: Johns Hopkins university center for systems science and engineering, Bull. Assoc. Can. Map Libr. Arch.(ACMLA) 164 (2020) (2019) 47–51.

[2] T. Ai, Z. Yang, H. Hou, C. Zhan, C. Chen, W. Lv, Q. Tao, Z. Sun, L. Xia, Correlation of chest CT and RT-PCR testing for coronavirus disease 2019 (COVID-19) in China: A report of 1014 cases, Radiology 296 (2) (2020) E32–E40.

[3] G. Castellano, L. Bonilha, L.M. Li, F. Cendes, Texture analysis of medical images, Clin. Radiol. 59 (12) (2004) 1061–1069.

[4] Y. Fang, H. Zhang, J. Xie, M. Lin, L. Ying, P. Pang, M. Ji, Sensitivity of chest CT for COVID-19: Comparison to RT-PCR, Radiology 296 (2) (2020) E115–E117.

[5] H.X. Bai, B. Hsieh, Z. Xiong, K. Halsey, J.W. Choi, T.M. Tran, I. Pan, L.B. Shi, D.C. Wang, J. Mei, X.L. Jiang, Performance of radiologists in differentiating COVID-19 from non-COVID-19 viral pneumonia at chest CT, Radiology 296 (2) (2020) E46–E54.

[6] T. Nihashi, T. Ishigaki, H. Satake, S. Ito, O. Kaii, Y. Mori, K. Shimamoto, H. Fukushima, K. Suzuki, H. Umakoshi, M. Ohashi, F. Kawaguchi, S. Naganawa, Monitoring of fatigue in radiologists during prolonged image interpretation using fNIRS, Jpn. J. Radiol. 37 (2019) 437–448.

[7] E.J. Mortani Barbosa, B. Georgescu, S. Chaganti, G.B. Aleman, J.B. Cabrero, G. Chabin, T. Flohr, P. Grenier, S. Grbic, N. Gupta, et al., Machine learning automatically detects covid-19 using chest CTs in a large multicenter cohort, Eur. J. Radiol. 31 (11) (2021) 8775–8785.

[8] S. Wang, B. Kang, J. Ma, X. Zeng, M. Xiao, J. Guo, M. Cai, J. Yang, Y. Li, X. Meng, B. Xu, A deep learning algorithm using CT images to screen for Corona Virus Disease (COVID-19), Eur. J. Radiol. 31 (8) (2021) 6096–6104.

[9] Y. Pathak, P.K. Shukla, A. Tiwari, S. Stalin, S. Singh, P.K. Shukla, Deep transfer learning based classification model for Covid-19 disease, IRBM (2020).

[10] A. Gudigar, U. Raghavendra, S. Nayak, et al., Role of artificial intelligence in COVID-19 detection, Sensors 21 (23) (2021) 8045.

[11] N. Subramanian, O. Elharrouss, S. Al-Maadeed, M. Chowdhury, A review of deep learning-based detection methods for COVID-19, Comput. Methods Programs Biomed. (2022) 105233.

[12] Y. Wan, H. Zhou, X. Zhang, An interpretation architecture for deep learning models with the application of COVID-19 diagnosis, Entropy 23 (2021) 204.

[13] X. Ouyang, J. Huo, L. Xia, F. Shan, J. Liu, Z. Mo, F. Yan, Z. Ding, Q. Yang, B. Song, et al., Dual-sampling attention network for diagnosis of COVID-19 from community acquired pneumonia, IEEE Trans. Med. Imaging 39 (2020) 2595–2605.

[14] M. Elpeltagy, H. Sallam, Automatic prediction of COVID-19 from chest images using modified ResNet50, Multimedia Tools Appl. (2021) 1–13.

[15] H. Hirano, K. Koga, K. Takemoto, Vulnerability of deep neural networks for detecting COVID-19 cases from chest X-ray images to universal adversarial attacks, PLoS One 15 (2020) e0243963.

[16] S. Sakib, T. Tazrin, M.M. Fouda, Z.M. Fadlullah, M. Guizani, DL-CRC: Deep learning-based chest radiograph classification for COVID-19 detection: A novel approach, IEEE Access 8 (2020) 171575–171589.

[17] C.B.S. Maior, J.M.M. Santana, I.D. Lins, M.J.C. Moura, Convolutional neural network model based on radiological images to support COVID-19 diagnosis: Evaluating database biases, PLoS One 16 (2021) e0247839.

[18] S. Dong, Q. Yang, Y. Fu, M. Tian, C. Zhuo, RCoNet: Deformable mutual information maximization and high-order uncertainty-aware learning for robust COVID-19 detection, IEEE Trans. Neural Netw. Learn. Syst. 32 (2021) 3401–3411.

[19] D.S. Kermany, M. Goldbaum, W. Cai, C.C.S. Valentim, H. Liang, S.L. Baxter, A. Mckeown, G. Yang, X. Wu, F. Yan, et al., Identifying medical diagnoses and treatable diseases by image-based deep learning, Cell 172 (5) (2018) 1122–1131.

[20] L. Torrey, J. Shavlik, Handbook of research on machine learning applications and trends: algorithms, methods, and techniques, IGI Global, 2009, pp. 242–264.

[21] H. Wang, S. Wang, Z. Qin, Y. Zhang, R. Li, Y. Xia, Triple attention learning for classification of 14 thoracic diseases using chest radiography, Med. Image Anal. 67 (2021) 101846.

[22] H. Li, C. Vong, P.K. Wong, W.F. Ip, T. Yan, I.C. Choi, H.H. Yu, A multi-feature fusion method for image recognition of gastrointestinal metaplasia (GIM), Biomed. Signal Process. Control 69 (2021) 102909.

[23] S. Ahuja, B.K. Panigrahi, N. Dey, T. Gandhi, V. Rajinikanth, Deep transfer learning-based automated detection of COVID-19 from lung CT scan slices, Appl. Intell. 51 (1) (2021) 571–585.

[24] P. gifani, A. Shalbaf, M. Vafaeezadeh, Automated detection of COVID-19 using ensemble of transfer learning with deep convolutional neural network based on CT scans, Int. J. CARS 16 (1) (2021) 115–123.

[25] K. Xu, J. Ba, R. Kiros, K. Cho, A. Courville, R. Salakhudinov, R. Zemel, Y. Bengio, Show, attend and tell: Neural image caption generation with visual attention, in: Proceedings of the 32nd International Conference on Machine Learning, ICML, 2015, pp. 2048–2057.

[26] F. Wang, M. Jiang, C. Qian, S. Yang, C. Li, H. Zhang, X. Wang, X. Tang, Residual attention network for image classification, in: Proceedings of the IEEE/CVF Conference on Computer Vision and Pattern Recognition, CVPR, 2017, pp. 3156–3164.

[27] T. Zhou, S. Canu, S. Ruan, Automatic COVID-19 CT segmentation using U-Net integrated spatial and channel attention mechanism, Int. J. Imaging Syst. Technol. (2020) 1–12.

[28] J. Wang, Y. Bao, Y. Wen, H. Lu, H. Luo, Y. Xiang, X. Li, C. Liu, D. Qian, Prior-attention residual learning for more discriminative COVID-19 screening in CT images, IEEE Trans. Med. Imaging 39 (8) (2020) 2572–2583.

[29] Y.D. Zhang, Z. Zhang, X. Zhang, S.H. Wang, MIDCAN: A multiple input deep convolutional attention network for Covid-19 diagnosis based on chest CT and chest X-ray, Pattern Recognit. Lett. 150 (2021) 8–16.

[30] H. Xia, M. Ma, H. Li, et al., MC-Net: multi-scale context-attention network for medical CT image segmentation, Appl. Intell. 52 (2) (2022) 1508–1519.

[31] C.L.P. Chen, Z. Liu, Broad learning system: an effective and efficient incremental learning system without the need for deep architecture, IEEE Trans. Neural Networks Learn. Syst. 29 (1) (2017) 10–24.

[32] C.L.P. Chen, Z. Liu, S. Feng, Universal approximation capability of broad learning system and its structural variations, IEEE Trans. Neural Netw. Learn. Syst. 30 (4) (2018) 1191–1204.

[33] Z. Liu, C.L.P. Chen, Broad learning system: Structural extensions on single-layer and multi-layer neural networks, in: Proc. SPAC, 2017, pp. 136–141.

[34] J. Jin, Z. Liu, C.L.P. Chen, Discriminative graph regularized broad learning system for image recognition, Sci. China Inf. Sci. 61 (11) (2018) 1–14.

[35] Y. Zhang, K. Yuen, Crack detection using fusion features-based broad learning system and image processing, Comput. Aided Civ. Infrastruct. Eng 36 (12) (2021) 1568–1584.

[36] P.K. Wong, L. Yao, T. Yan, I.C. Choi, H.H. Yu, Y. Hu, Broad learning system stacking with multi-scale attention for the diagnosis of gastric intestinal metaplasia, Biomed. Signal Process. Control 73 (2022) 103476.

[37] R. Han, Z. Liu, C.L.P. Chen, Multi-scale 3D convolution feature-based broad learning system for alzheimer's disease diagnosis via MRI images, Appl. Soft Comput. 120 (2022) 108660.

[38] S. Feng, C.L.P. Chen, Fuzzy broad learning system: A novel neuro-fuzzy model for regression and classification, IEEE Trans. Cybern. 50 (2) (2018) 414–424.

[39] J.W. Jin, C.L.P. Chen, Regularized robust broad learning system for uncertain data modeling, Neurocomputing 322 (2018) 58–69.

[40] L. Wang, Z.Q. Lin, A. Wong, COVID-Net: a tailored deep convolutional neural network design for detection of COVID-19 cases from chest X-ray images, Sci. Rep. 10 (2020) 19549.

[41] O. Gozes, M. Frid-Adar, H. Greenspan, P.D. Browning, H. Zhang, W. Ji, A. Bernheim, E. Siegel, Rapid AI development cycle for the coronavirus (covid-19) pandemic: Initial results for automated detection & patient monitoring using deep learning ct image analysis, 2020, arXiv:2003.05037.

[42] F. Shan, Y. Gao, J. Wang, W.Shi, N. Shi, M. Han, Z. Xue, D. Shen, Y. Shi, Lung infection quantification of COVID-19 in CT images with deep learning, 2020, arXiv preprint arXiv:2003.04655.

[43] D. Kollias, A. Arsenos, S. Kollias, Ai-mia: Covid-19 detection & severity analysis through medical imaging, 2022, arXiv preprint arXiv:2206.04732.

[44] L. Li, L. Qin, Z. Xu, Y. Yin, X. Wang, B. Kong, J. Bai, Y. Lu, Z. Fang, Q. Song, K. Cao, D. Liu, G. Wang, Q. Xu, X. Fang, S. Zhang, J. Xia, J. Xia, Artificial intelligence distinguishes COVID-19 from community acquired pneumonia on chest CT, Radiology (2020) 200905.

[45] D.P. Fan, T. Zhou, G.P. Ji, Y. Zhou, G. Chen, H. Fu, J. Shen, L. Shao, Inf-net:automatic covid-19 lung infection segmentation from CT images, IEEE Trans. Med. Imaging 39 (8) (2020) 2626–2637.

[46] K. He, X. Zhang, S. Ren, J. Sun, Deep residual learning for image recognition, in: Proceedings of the IEEE/CVF Conference on Computer Vision and Pattern Recognition, 2016, pp. 770–778.

[47] K. Zhang, X. Liu, J. Shen, Z. L, Y. S, X. W, et al., Clinically applicable AI system for accurate diagnosis, quantitative measurements, and prognosis of COVID-19 pneumonia using computed tomography, Cell 181 (6) (2020) 1423–1433.

[48] J. Zhao, Y. Zhang, X. He, P. Xie, Covid-CT-dataset: A CT scan dataset about Covid-19, 2020, arXiv preprint arXiv:2003.13865.

[49] E. Soares, P. Angelov, S. Biaso, M. Higa Froes, D. Kanda Abe, SARS-CoV-2 CT-scan dataset: A large dataset of real patients CT scans for SARS-CoV-2 identification, 2020, MedRxiv.

[50] K. Simonyan, A. Zisserman, Very deep convolutional networks for large-scale image recognition, 2014, arXiv preprint arXiv:1409.1556.

[51] F. Chollet, Xception: Deep learning with depthwise separable convolutions, in: Proc.IEEE Conf. Comp. Vis. Patt. Recogn, 2017, pp. 1251–1258.
[52] M. Tan, Q. Le, Efficientnet: Rethinking model scaling for convolutional neural networks, in: Proc. Int. Conf. Mach. Learn, 2019.
[53] J. Li, G. Zhao, Y. Tao, P. Zhai, H. Chen, H. He, T. Cai, Multi-task contrastive learning for automatic CT and X-ray diagnosis of COVID-19, Pattern Recognit. 114 (2021) 107848.
[54] A. Altan, S. Karasu, Recognition of COVID-19 disease from X-ray images by hybrid model consisting of 2D curvelet transform, chaotic salp swarm algorithm and deep learning technique, Chaos Solitons Fractals 140 (2020) 110071.
[55] A. Oluwasanmi, M.U. Aftab, Z. Qin, S.T. Ngo, T. Van Doan, S.B. Nguyen, Transfer learning and semisupervised adversarial detection and classification of COVID-19 in CT images, Complexity 2021 (2021) 6680455.